

Article

Graphene Xerogel for Drug Release

Kyriaki Kalyva, Katerina Michalarou , Moch Izzul Haq Al Maruf  and Vasilios I. Georgakilas * 

Department of Materials Science, University of Patras, 26504 Rio Achaia, Greece

* Correspondence: viegeorgaki@upatras.gr

Abstract: By functionalizing reduced graphene oxide with polydopamine, the production of a two-dimensional hydrophilic platform with hydrophobic areas, suitable for the stabilization and slow and controlled release of hydrophilic and hydrophobic drugs, was realized. The functionalized graphene was first enriched with different organic drug molecules, either hydrophilic, such as doxorubicin, or hydrophobic, such as curcumin or quercetin, and then incorporated into a xerogel of chitosan and polyvinyl alcohol. The graphene substrate stabilizes the xerogel in water and effectively controls the release of doxorubicin for more than three weeks. The release of curcumin and quercetin in the aqueous environment was equally successful but at different rates. The drug-loaded xerogels also worked effectively after their incorporation into a hemostatic cotton gauze.

Keywords: xerogel; drug delivery; drug release; quercetin; curcumin; polydopamine

1. Introduction

Polydopamine (PDA) is a fascinating bioinspired polymer [1] that has the unique ability to form thin films covering almost all kinds of surfaces and exhibits remarkable adhesive properties [2–4]. It is easily formed by the self-polymerization of dopamine in alkaline water solutions. It has been used in many applications such as in energy, catalysis, water treatment, or sensing [5]. Due to its biocompatibility, it has been used for coating surfaces for bioapplications [6–9]. Although several attempts have been made up to now, the exact structure of PDA remains unknown [10]. Among all else, PDA has proven very effective for the functionalization of GO for several applications such as absorbent, corrosion properties, membranes, and water desalination [11–18].

GO, being the oxidized form of graphene, has a limited aromatic character and is rich in oxygen groups such as hydroxyls, carboxylates, and epoxy which give graphene a hydrophilic character and considerable stability in a water dispersion [19]. With the reduction of GO, the aromatic character is partially recovered, and the oxygen groups are largely removed. The result is that the reduced graphene oxide (rGO) loses its hydrophilic character and becomes an amphiphilic derivative [20,21]. In this way, it forms aggregates and traps quantities of water, resulting in the formation of hydrogels. Often these hydrogels resulting from the reduction of the GO are reinforced with polymers [22], biopolymers [23], and other materials to enrich their properties and use them as biomaterials [22–24].

Graphene hydrogels can be converted into aerogels by lyophilization or xerogels by physical air-drying. Graphene aerogels have a stable structure, significant porosity, high specific surface area, and have been used in the removal of heavy metals, in batteries, sensors and biosensors. The formation of graphene hydrogels and aerogels is one of the most widespread uses of GO [25,26]. Our group has described the formation of graphene aerogels doped with diamines and aerogels reinforced with carbon fibers [27–29].

Poly(vinyl) alcohol (PVA) is a water-soluble polymer; very widespread and often used for hydrogels. PVA-based hydrogels have low toxicity and good biocompatibility, high water absorption, and remarkable mechanical properties. It has been extensively studied as a drug carrier, for wound healing, tissue engineering, and bioapplications [30–32].



Citation: Kalyva, K.; Michalarou, K.; Maruf, M.I.H.A.; Georgakilas, V.I. Graphene Xerogel for Drug Release. *C* **2024**, *10*, 99. <https://doi.org/10.3390/c10040099>

Academic Editor: Giuseppe Cirillo

Received: 1 October 2024

Revised: 16 November 2024

Accepted: 20 November 2024

Published: 28 November 2024



Copyright: © 2024 by the authors. Licensee MDPI, Basel, Switzerland. This article is an open access article distributed under the terms and conditions of the Creative Commons Attribution (CC BY) license (<https://creativecommons.org/licenses/by/4.0/>).

PVA has, among others, been combined with chitosan, which provides the hydrogel with antibacterial properties and thermal and mechanical stability [33,34]. Chitosan is one of the most interesting biopolymers with antimicrobial, antifungal, and hemostatic properties. It is a polysaccharide of natural origin and has been extensively studied in biopharmaceuticals, with most interest in wound healing [35]. Chitosan has often been reinforced with carbon nanotubes and graphene oxide nanosheets. Carbon nanostructures enhance the mechanical properties of the composite and, thanks to their electrical conductivity, can promote nerve regeneration in deep wounds [36,37]. Graphene oxide possesses several functional oxygen groups such as hydroxyls, carboxyls, and epoxies, with which it can significantly promote as a crosslinker chitosan network formation [38].

In this article, we describe the formation of a xerogel from chitosan and polyvinyl alcohol reinforced with polydopamine-functionalized graphene (rGO-PDA) as substrate and its use for the drug loading and slow release. The drug-loaded xerogel could be used for the transdermal administration of drugs or therapeutic agents. As representative substances that can be delivered by this rGO-PDA-doped xerogel, doxorubicin, quercetin, and curcumin have been selected. The substances are incorporated into the graphene platform and then covered by the polymer blends of the hydrogel. The product is stabilized in the form of xerogel and can be converted back to a hydrogel before use, releasing therapeutic substances on contact with the skin. Alternatively, hydrogel can be easily incorporated into fabric, which, in the form of wearable patches, can provide a good fit on various parts of the human body for continuous contact with the skin and transdermal delivery over long periods of time [39]. For this reason, here the xerogel was embedded in a cotton gauze and the drug release was examined by immersing the gauze in water.

The introduction of pharmaceutical substances into the human body is an important issue that seriously affects the effectiveness of the drug. Transdermal administration is an alternative method of drug delivery through the skin via a diffusion process into the bloodstream and, from there, to the target organs. This method has significant advantages, such as continuous and controlled drug administration, avoidance of digestion and metabolism in the liver, and limited toxicity. However, up to now it has been used mainly for substances that can penetrate the outer layer of the skin (stratum corneum) [40].

Doxorubicin is a widely used anti-cancer chemotherapeutic drug that acts by blocking DNA replication in solid tumors like breast, lung, and skin cancers. Since its action takes place in the nucleus of cancer cells, the efficient action requires its effective transport to the cell nucleus. Usually, it is administered in doses by intravenous injections, causing many side effects such as alopecia, myelosuppression, mouth ulcers, and cardiotoxicity that limit its clinical application. To avoid this limitation, several efforts have been made to use transdermal administration of DOX [41–43].

Curcumin is a natural herbal product traditionally used for wound healing [44] and its anti-inflammatory and antioxidant properties. It is a polyphenolic compound from the rhizome of *Curcuma longa*, quite hydrophobic and poorly soluble in aqueous media. It is often used for the transdermal therapy of psoriasis, using liposomes or hydrogels to overcome its poor solubility in water [45–49]. Much research has also been devoted to its therapeutic potential in breast cancer prevention. However, due to its poor absorption when consumed orally, the anticancer effects of curcumin have not yet been fully exploited. Atlan et al. proposed a curcumin-modified textile product that offers transdermal, targeted drug delivery simply through skin contact for daily breast cancer prevention [30].

Quercetin is another polyphenol of natural origin from the flavonol family with high therapeutic potential [50], but limited pharmacological use due to its low water solubility and bioavailability [51]. It has been shown that quercetin can be transported through the skin using mesoporous silica particles, embedded in oleogel [52].

2. Materials and Methods

2.1. Materials

Graphite, curcumin (Curc), polyvinyl alcohol (PVA), and dopamine were purchased from Alfa Aesar Thermo Fisher Scientific, Waltham, MA, USA; doxorubicin hydrochloride (DOX) from Merck & Co., Inc., Rahway, NJ, USA; quercetin hydrate (Querc) from Cayman Chemical Company, Ann Arbor, MI, USA; chitosan (Chit) from Glentham Life Sciences Ltd., Wiltshire, UK. All other chemicals and solvents were of analytical grade.

2.2. Preparation of GO

GO was prepared according to Staudenmaier's method (Staudenmaier, 1898) through oxidation of graphite [39,53]. 20 g of graphite was added to 600 mL of a cold mixture of H₂SO₄ and HNO₃, (2:1). 200 g of KClO₃ powder was added to the cold mixture in small portions under continuous stirring. The reaction was quenched after 20 h by pouring the mixture into deionized water. The GO product was then washed until the pH reached 6.0 and was dried at room temperature.

2.3. Preparation of rGO-PDA

50 mg of GO was mixed with an excess of dopamine (200 mg) in 50 mL of water and the pH was controlled to 8.5 with concentrated ammonia. The mixture was stirred overnight, and the product was isolated with centrifugation and filtration (hydrophilic membrane filter 0.2 µm) and washed with water.

2.4. Preparation of Hydrogel rGO-PDA

50 mg of PVA and 10 mg of Chit were dissolved in 1 mL of water and stirred overnight. The PVA/Chit mixture was then mixed with 1 mL of rGO-PDA (1 g L⁻¹), deposited on a glass slide, and air-dried. For the study of the xerogel as a drug release system, a quantity of doxorubicin (DOX) was first incorporated into the rGO-PDA.

2.5. Preparation of Hydrogel rGO-PDA/DOX

250 µL of DOX solution (1 g L⁻¹) was mixed with 1 mL rGO-PDA (1 g L⁻¹) and stirred overnight. The mixture was then added to 1 mL of PVA/Chit solution, and half of the product was deposited on glass and air-dried. The control sample contains the same quantities, except the rGO-PDA.

2.6. Preparation of Hydrogel rGO-PDA/Querc

100 µL of Quercetin solution (2 g L⁻¹) in ethanol was mixed with 1 mL rGO-PDA (1 g L⁻¹) and stirred overnight. The mixture was then added to 1 mL of PVA/Chit solution, and half of the product was embedded in a piece of gauze and air-dried.

2.7. Preparation of Hydrogel rGO-PDA/Curc

100 µL of Curcumin solution (2 g L⁻¹) in ethanol was mixed with 1 mL rGO-PDA (1 g L⁻¹) and stirred overnight. The mixture was then added to 1 mL of PVA/Chit solution and half of the product was embedded in a piece of gauze and air-dried.

2.8. Characterization Methods

The FTIR spectra were performed with an ATR technique on a Fourier transform spectrometer (IRTracer-100, Shimadzu Europa GmbH, Duisburg, Germany). The optical spectra were recorded in water dispersion with a Shimadzu UV-1900 (Shimadzu, Duisburg, Germany).

DLS and PDI. The determination of the hydrodynamic diameter and polydispersity index (PDI) of nanoparticles dispersed in water was performed in a ZetaSizer Nano series Nano-ZS (Malvern Instruments Ltd., Malvern, UK) equipped with a He-Ne laser beam at a wavelength of 633 nm and a fixed backscattering angle of 173°. Polydispersity index (PDI)

is the square of light scattering polydispersity and indicates the size distribution of the size of the nanosheets.

3. Results and Discussion

The treatment of GO with dopamine in alkaline water dispersion resulted in the partial reduction of GO and the functionalization with polydopamine. The product rGO-PDA can be seen as a biocompatible, two-dimensional (2D) platform with aromatic moieties and PDA oligomers or macromolecules attached to the surface. Although not yet fully explained, the PDA aromatic parts and NH or OH groups could provide covalent bonds or van der Waals interactions and hydrogen bonds as the main attractive forces that bind PDA to rGO [54]. rGO-PDA was highly hydrophilic and formed stable dispersion in water (see Figure 1). Based on the mass of the product that was isolated and the starting amount of GO, the PDA percentage in rGO-PDA was estimated to be approximately 35%. To form the xerogel, rGO-PDA was mixed with a mixture of chitosan and PVA, deposited on a glass slide, and air-dried. The removal of water from the hydrogel by evaporation results in significant shrinkage of the structure and the formation of a xerogel in the form of a stable film with significant mechanical stability. The XRD pattern of the xerogel showed a totally amorphous phase, indicating a homogeneous dispersion of the rGO-PDA in the polymer blend. Microscopic analysis of the xerogel film by SEM analysis showed the absence of pores on the surface. However, on contact of the film with water, the hydrogel is regenerated and then studied as a drug release system.

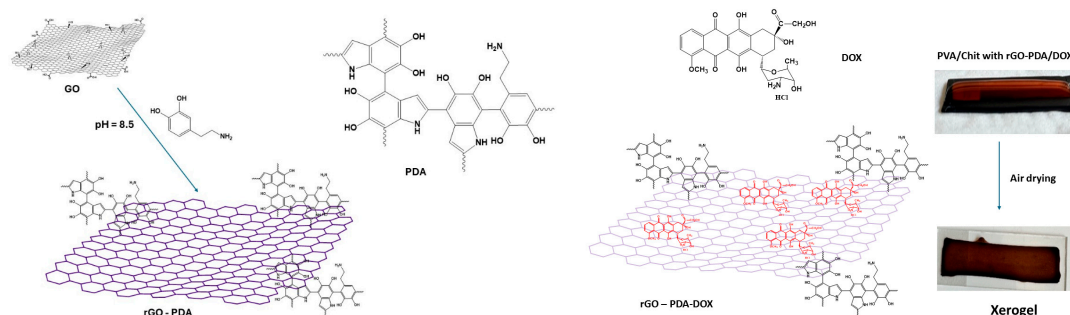


Figure 1. The formation of the rGO-PDA derivative and attachment of DOX (red colored) on rGO-PDA (rGO-PDA/DOX).

Firstly, DOX was selected as a representative hydrophilic compound to be loaded and released from the hydrogel. A quantity of DOX was incorporated into the rGO-PDA. Due to the solubility of DOX in water, both components were mixed in water. The DOX molecules interact mainly with the aromatic areas of the graphene by π stacking interactions (see Figure 1) as well as with OH and NH groups of PDA by hydrogen bonds [55,56]. Curcumin (Curc) and quercetin (Querc) are hydrophobic substances and thus are not sufficiently soluble in water. Therefore, the deposition of those compounds on the rGO-PDA surface was performed in an ethanol/water mixture. Both compounds have aromatic rings that favor their hydrophobicity and contribute to the van der Waals interactions with the graphene platforms through π stacking, and oxygen groups that can be involved with hydrogen bonds with PDA chains [57–60]. The prepared hybrids rGO-PDA/drug were then incorporated into the PVA-chitosan blend, forming hydrogels and the final xerogels. The presence of rGO-PDA nanosheets provides a significant mechanical stability to the hydrogels, and thus maintaining their structure even after 30 days in water. Whereas hydrogels without rGO-PDA nanosheets that were used in control experiments have much less stability and are often destroyed much faster in water.

The FT-IR spectrum of rGO-PDA has some different peaks compared to that of GO due to the addition of PDA groups on the graphene surface and the removal of oxygen groups from GO by the reductive action of dopamine. The spectrum of GO has some characteristic peaks at $3000\text{--}3400\text{ cm}^{-1}$ (ν_{OH}), 1620 cm^{-1} (C=C stretching and water bending), 1370 cm^{-1} (C-OH

bending), 1190 (epoxy or S=O stretching), and 1043 (C-OH stretching), 980 cm^{-1} (epoxy stretching) [61]. The spectrum of rGO-PDA has much lower peaks in the 3000–3400 region and 1620 cm^{-1} due to the removal of oxygen groups, with new peaks at 1500 and 1580 cm^{-1} that correspond to the N-H bonding and C=C stretching vibration respectively (see Figure 2a) [62,63]. The characteristic peak of N-H at around 3100 cm^{-1} is very broad due to hydrogen bond interaction and therefore difficult to observe [64,65].

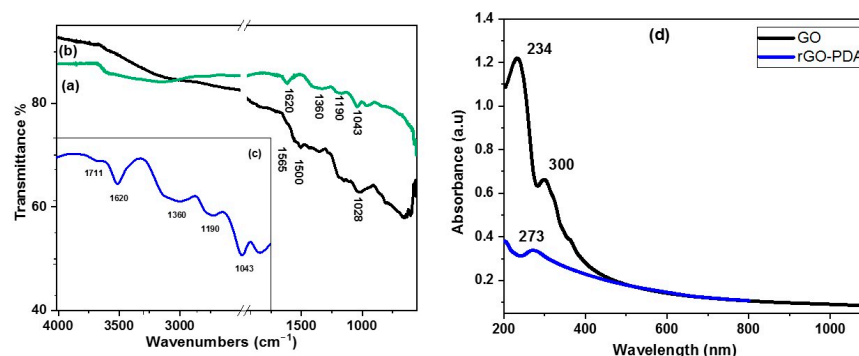


Figure 2. FTIR spectra of (a) GO, (b) rGO-PDA (c) Part of the spectrum (a) in magnification. and (d) UV-Vis spectra of GO and rGO-PDA dispersed in water.

The UV-Vis spectrum of GO has a band with two distinct λ_{max} at 234 and 300 nm due to π, π^* and n, π^* transitions. In the spectrum of rGO-PDA, the peak at 300 nm was removed, indicating the absence of oxygen groups, and the π, π^* transition was red-shifted to 273 nm due to increased aromaticity of the product after the reduction of GO (see Figure 2b) [66]. The dynamic light scattering (DLS) of rGO-PDA (see Figure 3) showed a mean size of the particle of about 300 nm, with a zeta potential of -21.6 mV, showing that the colloidal stability of the product in water was partly attributed to the charge of the surface [67]. The polydispersity index (PDI) was measured to 0.42, indicating a moderate size distribution of the rGO-PDA nanosheets.

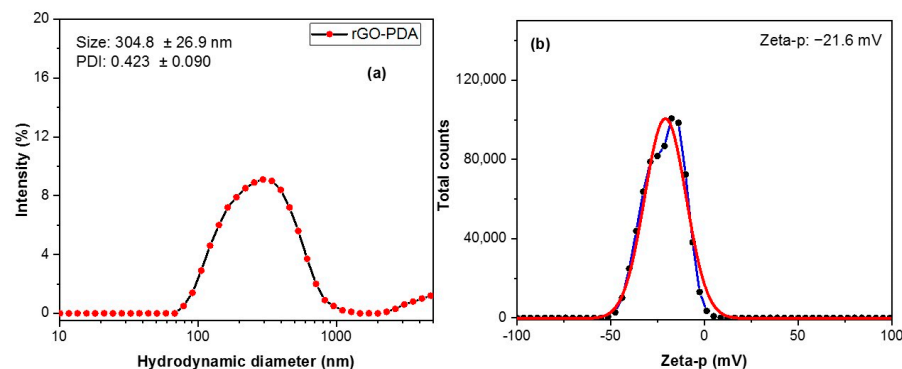


Figure 3. (a) DLS analysis and (b) zeta potential of rGO-PDA (the red line represent Gauss fitting).

3.1. Release of DOX from Hydrogel and Gauze with Embedded Hydrogel

DOX was embedded into the xerogel by mixing it with rGO-PDA in the first stage. DOX molecules were absorbed onto the surfaces of rGO-PDA nanosheets through van der Waals interactions, as indicated by the discoloration of the DOX solution after the addition of rGO-PDA and overnight stirring. Furthermore, the UV-Vis absorption of DOX was less intense after the addition of rGO-PDA, and at least two of its bands were shifted due to the interaction with the surface of rGO-PDA (see Figure 4d). The xerogel rGO-PDA/DOX and blank samples, in the form of dry films, contained 125 μg of DOX and were kept in the dark. For the release experiments, the samples were placed in water. The xerogels absorbing water were converted to hydrogel and started releasing DOX. The amount of DOX released as a function of days is shown in Figure 4. The blank sample (without rGO-PDA) released a

total of approximately 71 μg of DOX after 11 days, with 90% (64 μg) of this amount released in the first two days. The sample with rGO-PDA released approximately 90 μg of DOX after 33 days, with only 56% (49 μg) of this amount released on the first day. After day 9, the sample released about 0.4 μg on average each day.

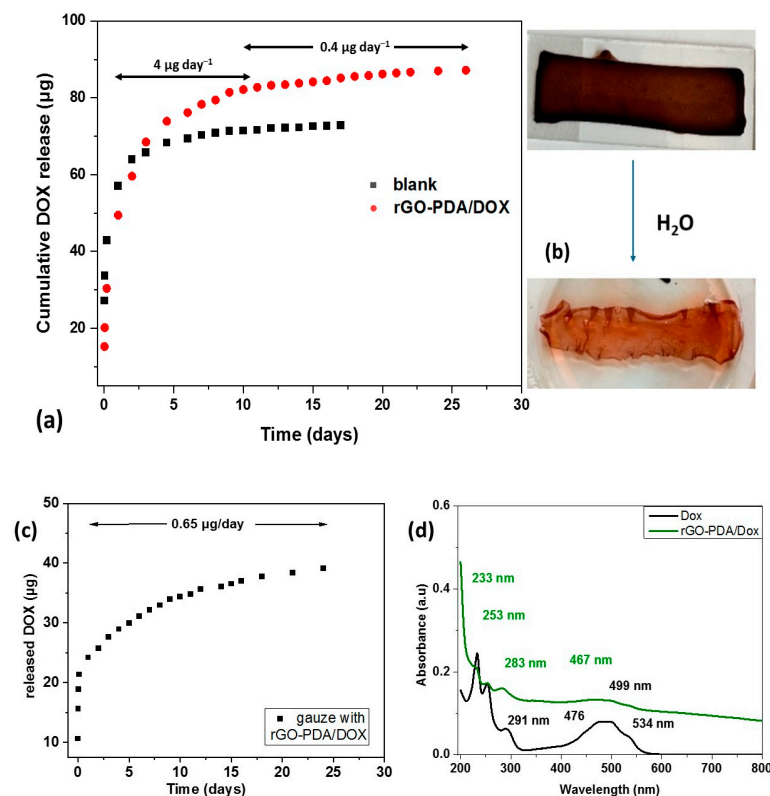


Figure 4. (a) The released amount of DOX per day from rGO-PDA/DOX hydrogel, (b) photo of the DOX-doped xerogel before and after the release process, (c) the release of DOX per day from the gauze modified with rGO-PDA/DOX hydrogel, (d) the UV-Vis spectra of DOX and rGO-PDA/DOx hybrid.

The rGO-PDA/DOX hydrogel was then incorporated into a gauze and air-dried. The gauze embedded with rGO-PDA/DOX was placed in water to measure the release of DOX. The total amount of DOX incorporated in the gauze sample was 62.5 μg . During the release process, about 24 μg (61% of the total released amount) was released on the first day, while the next 15 μg of DOX was released slowly over 22 days. By comparing the two different release procedures—hydrogel and gauze with embedded hydrogel—it is observed that after the first day, where both procedures release similar amounts of approximately 60%, the gauze has a smoother release over the whole period from day 2 to day 22 (average release 0.65 $\mu\text{g/day}$), while the hydrogel initially releases the drug at a higher rate (average release 4 $\mu\text{g/day}$) for 8 days and then at a lower rate (average release 0.4 $\mu\text{g/day}$). The smooth release of DOX from the gauze can be correlated with the increased surface of the hydrogel that is absorbed into the cotton textile.

3.2. Release of Quercetin from Gauze with Embedded Hydrogel

Quercetin was first embedded into the rGO-PDA nanosheets. The aromatic part of the molecules, as well as the oxygen groups they contain, ensure that the quercetin molecules are attached to the nanosheets through van der Waals interactions and hydrogen bonds. These interactions are responsible for the red shift of the two characteristic bands in the UV-Vis spectrum of rGO-PDA/Querc compared to free quercetin (see Figure 5a). Afterwards, the rGO-PDA/Querc hydrogel was incorporated into a gauze and air-dried. For the release measurements, the rGO-PDA/Querc-embedded gauze was placed in water. The total amount of the drug that was incorporated into a gauze sample was 50 μg . In a

period of 12 days, about 10 μg was released, although quercetin has very low solubility in water. About 6 μg was released on the first day, while the next 4 μg of the drug was released slowly over 12 days, with a mean amount of about 0.33 μg of quercetin every day (see Figure 5).

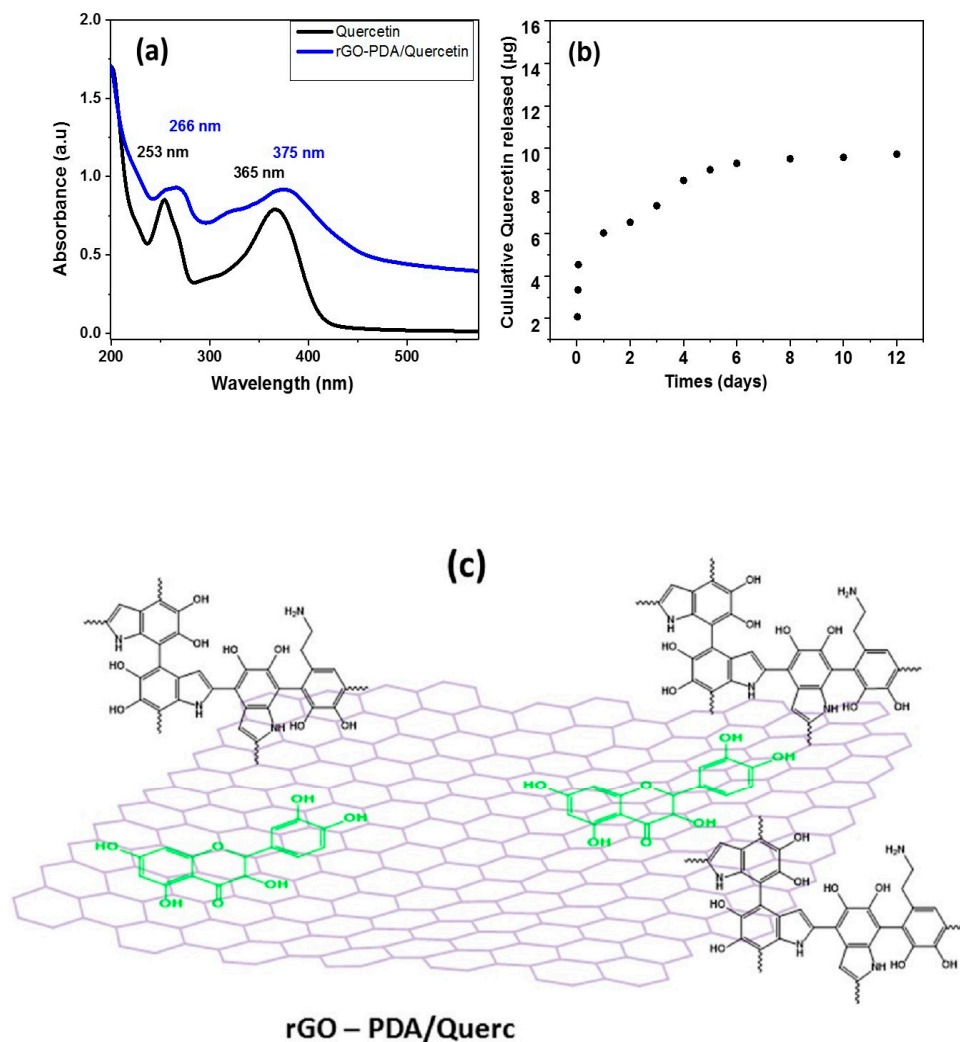


Figure 5. (a) The UV-Vis spectra of quercetin and rGO-PDA/Querc, (b) the release amount of quercetin per day from the gauze embedded with rGO-PDA/Querc hydrogel, (c) the suggested structure of rGO-PDA/Querc. (Querc is green colored).

3.3. Release of Curcumin from Gauze with Embedded Hydrogel

Curcumin was also first embedded into the rGO-PDA nanosheets before the hydrogel formation by overnight stirring in a water solution. Similar to the previous molecules, curcumin was strongly attached to the nanosheets through van der Waals interactions and hydrogen bonds due to its aromatic rings and the oxygen groups. The UV-Vis spectrum of rGO-PDA/Querc showed a less intense and broader band at 426 nm compared to the spectrum of free curcumin (see Figure 6d). The rGO-PDA/Querc embedded gauze was placed in water to measure the release of curcumin. The total amount of the drug that was incorporated into the gauze sample was 50 μg . During the release process, about 3 μg was released slowly over the first 7 days, with a mean amount of about 0.36 μg of curcumin every day, while the next 1 μg of the drug was released slowly over 10 days, at a mean amount of about 0.06 μg every day (see Figure 6).

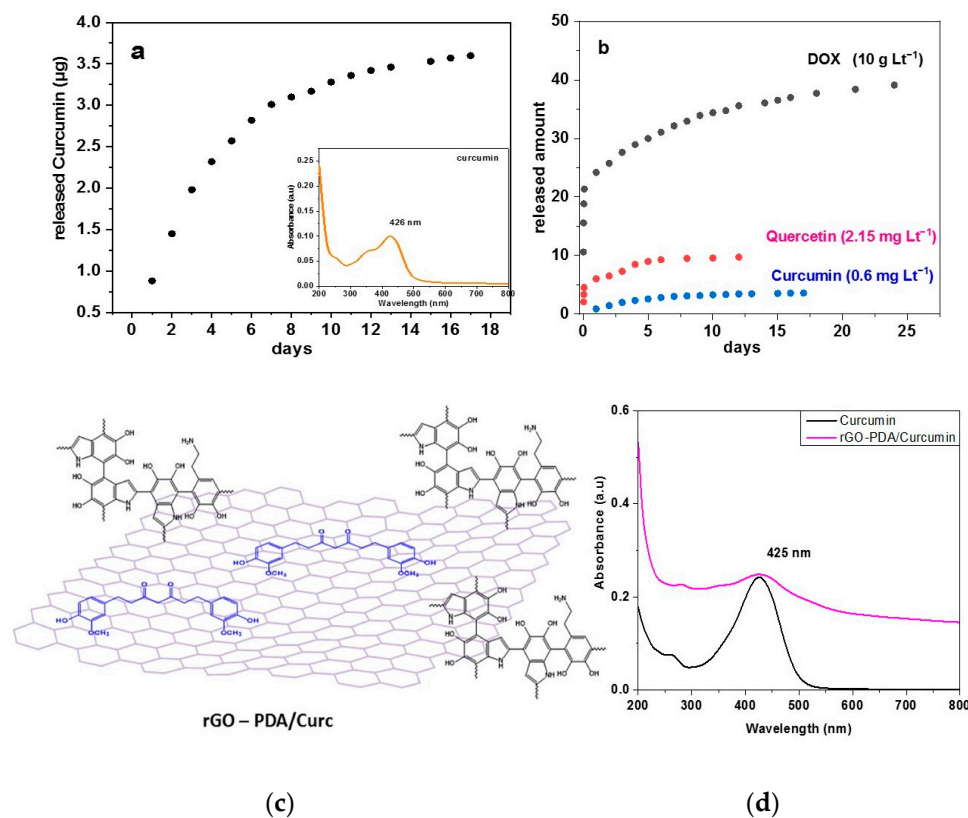


Figure 6. (a) The release amount of curcumin per day from the gauze embedded with rGO-PDA/Curc hydrogel, (b) comparison of the drug release from the gauze embedded with the rGO-PDA hydrogels between the three drug substances, (c) the suggested structure of rGO-PDA/Curc, where Curc are blue colored, (d) the UV-Vis spectra of free curcumin and rGO-PDA/Curc.

The gauze samples embedded with the drug-loaded hydrogels showed different release rates, which were mainly related to the solubility of the drug in water. DOX, with the higher water solubility (10 g L^{-1}), was released from the gauze at a rate of 39%, with an average of 0,65% per day. Quercetin, with much lower solubility (2.15 mg L^{-1}) was released at 20%, with an average of 0.33% per day, while curcumin, having the lowest solubility (0.6 mg L^{-1}), was released at 7%, with an average of 0.06% per day. DOX, having aromatic rings that help its anchoring to the surface of graphene but also hydrophilic groups that overlap overall, is gradually released from the surface of the graphene, through water, over a long period of about 3 weeks. The remaining two substances, quercetin and curcumin, are dominated by their hydrophobic character, which allows a stronger binding to the graphene surface, and this is reflected in the low release rate they exhibit. However, despite their low solubility in water, both compounds are released gradually over a period of about 2 weeks.

4. Conclusions

In this work, a graphene-based hydrogel rGO-PDA was constructed that can gradually release a hydrophilic substance like DOX for more than 1 month, without destroying its structure. For better application, the hydrogel was incorporated into a cotton gauze patch, where the release of DOX was similar in regards to the yield and the rate of the daily release. Furthermore, the hydrogel rGO-PDA embedded in gauze was suitable for the binding and release of hydrophobic substances such as quercetin and curcumin. The yield and the release rate of these substances were much lower due to their low solubility in water and stronger binding with the graphene surface.

Author Contributions: Conceptualization, V.I.G.; methodology, K.K., K.M. and M.I.H.A.M.; investigation, K.K., K.M. and M.I.H.A.M.; writing—original draft preparation, V.I.G.; writing—review and editing, V.I.G.; visualization, V.I.G.; supervision, V.I.G. All authors have read and agreed to the published version of the manuscript.

Funding: This research received no external funding.

Data Availability Statement: Data is contained within the article.

Conflicts of Interest: The authors declare no conflicts of interest.

References

1. Lee, H.; Dellatore, S.M.; Miller, W.M.; Messersmith, P.B. Mussel-inspired surface chemistry for multifunctional coatings. *Science* **2007**, *318*, 426–430. [[CrossRef](#)] [[PubMed](#)]
2. Hemmatpour, H.; De Luca, O.; Crestani, D.; Stuart, M.C.A. New insights in polydopamine formation via surface adsorption. *Nat. Commun.* **2023**, *14*, 664. [[CrossRef](#)] [[PubMed](#)]
3. Mei, H.; Gao, Z.; Wang, Q.; Sun, H.; Zhao, K.; Zhang, P.; Hao, J.; Ashokkumar, M.; Cui, J. Ultrasound expands the versatility of polydopamine coatings. *Ultrason. Sonochemistry* **2021**, *74*, 10571. [[CrossRef](#)] [[PubMed](#)]
4. Ryu, J.H.; Messersmith, P.B.; Lee, H. Polydopamine surface chemistry: A decade of discovery. *ACS Appl. Mater. Interfaces* **2018**, *10*, 7523–7540. [[CrossRef](#)] [[PubMed](#)]
5. Liu, Y.; Ai, K.; Lu, L. Polydopamine and Its Derivative Materials: Synthesis and Promising Applications in Energy, Environmental, and Biomedical Fields. *Chem. Rev.* **2014**, *114*, 5057–5115. [[CrossRef](#)] [[PubMed](#)]
6. Liang, Y.; Zhao, X.; Hu, T.; Han, Y.; Guo, B. Mussel-inspired, antibacterial, conductive, antioxidant, injectable composite hydrogel wound dressing to promote the regeneration of infected skin. *J. Colloid Interface Sci.* **2019**, *556*, 514–528. [[CrossRef](#)] [[PubMed](#)]
7. Wang, L.H.; Ernst, A.U.; An, D.; Datta, A.K.; Epel, B.; Kotecha, M.; Ma, M. A bio inspired scaffold for rapid oxygenation of cell encapsulation systems. *Nat. Commun.* **2021**, *12*, 5846. [[CrossRef](#)]
8. Cheng, W.; Zeng, X.; Chen, H.; Li, Z.; Zeng, W.; Mei, L.; Zhao, Y. Versatile polydopamine platforms: Synthesis and promising applications for surface modification and advanced nanomedicine. *ACS Nano* **2019**, *13*, 8537–8565. [[CrossRef](#)]
9. Yan, J.; Wu, R.; Liao, S.; Jiang, M.; Qian, Y. Applications of Polydopamine-Modified Scaffolds in the Peripheral Nerve Tissue Engineering. *Front. Bioeng. Biotechnol.* **2020**, *8*, 590998. [[CrossRef](#)]
10. Lyu, Q.; Hsueh, N.; Chai, C.L. Unravelling the polydopamine mystery: Is the end in sight? *Polym. Chem.* **2019**, *10*, 5771–5777. [[CrossRef](#)]
11. Song, X.; Lin, L.; Rong, M.; Wang, Y.; Xie, Z.; Chen, X. Mussel-inspired, ultralight, multifunctional 3D nitrogen-doped graphene aerogel. *Carbon* **2014**, *80*, 174–182. [[CrossRef](#)]
12. Zhang, X.; Nan, X.; Shi, W.; Sun, Y.; Su, H.; He, Y.; Liu, X.; Zhang, Z.; Ge, D. Polydopamine-functionalized nanographene oxide: A versatile nanocarrier for chemotherapy and photothermal therapy. *Nanotechnology* **2017**, *28*, 295102. [[CrossRef](#)] [[PubMed](#)]
13. Zhao, Z.; Li, J.; Wen, T.; Shen, C.; Wang, X.; Xu, A. Surface functionalization graphene oxide by polydopamine for high affinity of radionuclides. *Colloids Surf. A Physicochem. Eng. Asp.* **2015**, *482*, 258–266. [[CrossRef](#)]
14. Zhao, Z.; Guo, L.; Feng, L.; Lu, H.; Xu, Y.; Wang, J.; Xiang, B.; Zou, X. Polydopamine functionalized graphene oxide nanocomposites reinforced the corrosion protection and adhesion properties of waterborne polyurethane coatings. *Eur. Polym. J.* **2019**, *120*, 109249. [[CrossRef](#)]
15. Alkhouzaam, A.; Qiblawey, H.; Khraisheh, M. Polydopamine Functionalized Graphene Oxide as Membrane Nanofiller: Spectral and Structural Studies. *Membranes* **2021**, *11*, 86. [[CrossRef](#)] [[PubMed](#)]
16. Li, G.; Liang, Y.; Xu, C.; Sun, H.; Tao, L.; Wei, Y.; Wang, X. Polydopamine reinforced hemostasis of a graphene oxide sponge via enhanced platelet stimulation. *Colloids Surf. B Biointerfaces* **2019**, *174*, 35–41. [[CrossRef](#)]
17. Wang, J.; Huang, T.; Zhang, L.; Yu, Q.J.; Hou, L. Dopamine crosslinked graphene oxide membrane for simultaneous removal of organic pollutants and trace heavy metals from aqueous solution. *Environ. Technol.* **2017**, *39*, 3055–3065. [[CrossRef](#)]
18. Xu, K.; Feng, B.; Zhou, C.; Huang, A. Synthesis of highly stable graphene oxide membranes on polydopamine functionalized supports for seawater desalination. *Chem. Eng. Sci.* **2016**, *146*, 159–165. [[CrossRef](#)]
19. Chen, D.; Feng, H.; Li, J. Graphene Oxide: Preparation, Functionalization, and Electrochemical Applications. *Chem. Rev.* **2012**, *112*, 6027–6053. [[CrossRef](#)]
20. Razaq, A.; Bibi, F.; Zheng, X.; Papadakis, R.; Jafri, S.H.M.; Li, H. Review on Graphene, Graphene Oxide, Reduced Graphene Oxide-Based Flexible Composites: From Fabrication to Applications. *Materials* **2022**, *15*, 1012. [[CrossRef](#)]
21. Anegebe, B.; Ifijen, I.H.; Maliki, M.; Uwidia, I.E.; Aigbodion, A.I. Graphene oxide synthesis and applications in emerging contaminant removal: A comprehensive review. *Environ. Sci. Eur.* **2024**, *36*, 15. [[CrossRef](#)]
22. Yang, J.; Zhang, E.; Li, X.; Zhang, Y.; Qu, J.; Yu, Z.Z. Cellulose/graphene aerogel supported phase change composites with high thermal conductivity and good shape stability for thermal energy storage. *Carbon* **2016**, *98*, 50–57. [[CrossRef](#)]
23. Barra, A.; Santos, J.D.C.; Silva, M.R.F.; Nunes, C.; Ruiz-Hitzky, E.; Gonçalves, I.; Yildirim, S.; Ferreira, P.; Marques, P.A.A.P. Graphene Derivatives in Biopolymer-Based Composites for Food Packaging Applications. *Nanomaterials* **2020**, *10*, 2077. [[CrossRef](#)]

24. Pinelli, F.; Nespoli, T.; Rossi, F. Graphene Oxide-Chitosan Aerogels: Synthesis, Characterization, and Use as Adsorbent Material for Water Contaminants. *Gels* **2021**, *7*, 149. [[CrossRef](#)]
25. Li, Y.; Samad, Y.; Polychronopoulou, K.; Alhassan, S.M.; Liao, K. Highly Electrically Conductive Nanocomposites Based on Polymer Infused Graphene Sponges. *Sci. Rep.* **2014**, *4*, 4652.
26. Nassar, G.; Daou, E.; Najjar, R.; Bassil, M.; Habchi, R. A review on the current research on graphene-based aerogels and their applications. *Carbon Trends* **2021**, *4*, 100065. [[CrossRef](#)]
27. Wang, Z.; Liu, L.; Zhang, Y.; Huang, Y.; Liu, J.; Zhang, X.; Liu, X.; Teng, H.; Zhang, X.; Zhang, J.; et al. A Review of Graphene-Based Materials/Polymer Composite Aerogels. *Polymers* **2023**, *15*, 1888. [[CrossRef](#)] [[PubMed](#)]
28. Vrettos, K.; Angelopoulou, P.; Papavasiliou, J.; Avgouropoulos, G.; Georgakilas, V. Sulfur-doped graphene aerogels reinforced with carbon fibers as electrode materials. *J. Mater. Sci.* **2020**, *55*, 9676–9685. [[CrossRef](#)]
29. Vrettos, K.; Spyrou, K.; Georgakilas, V. Graphene Aerogel Growth on Functionalized Carbon Fibers. *Molecules* **2020**, *25*, 1295. [[CrossRef](#)]
30. Wang, M.; Bai, J.; Shao, K.; Tang, W.; Zhao, X.; Lin, D.; Huang, S.; Chen, C.; Ding, Z.; Ye, J. Poly(vinyl alcohol) Hydrogels: The Old and New Functional Materials. *Int. J. Polym. Sci.* **2021**, *2021*, 2225426. [[CrossRef](#)]
31. Liang, X.; Zhong, H.J.; Ding, H.; Yu, B.; Ma, X.; Liu, X.; Chong, C.M.; He, J. Polyvinyl Alco-hol (PVA)-Based Hydrogels: Recent Progress in Fabrication, Properties, and Multifunc-tional Applications. *Polymers* **2024**, *16*, 2755. [[CrossRef](#)] [[PubMed](#)]
32. Bercea, M. Recent Advances. in Poly(vinyl alcohol)-Based Hydrogels. *Polymers* **2024**, *16*, 2021. [[CrossRef](#)] [[PubMed](#)]
33. Farzinfar, E.; Paydayesh, A. Investigation of polyvinyl alcohol nanocomposite hydrogels containing chitosan nanoparticles as wound dressing. *Int. J. Polym. Mater. Polym. Biomater.* **2018**, *68*, 628–638. [[CrossRef](#)]
34. Kalantari, K.; Mostafavi, E.; Saleh, B.; Soltantabar, P.; Webster, T.J. Chitosan/PVA hydrogels incorporated with green synthesized cerium oxide nanoparticles for wound healing applications. *Eur. Polym. J.* **2020**, *134*, 109853. [[CrossRef](#)]
35. Mallakpour, S.; Azadia, E.; Hussain, C.M. Chitosan/carbon nanotube hybrids: Recent progress and achievements for industrial applications. *New J. Chem.* **2021**, *45*, 3756. [[CrossRef](#)]
36. Moradi, S.; Hamed, H.; Tonelli, A.E.; King, M.W. Chitosan/Graphene Oxide Composite Films and Their Biomedical and Drug Delivery Applications: A Review. *Appl. Sci.* **2021**, *11*, 7776. [[CrossRef](#)]
37. Khan, M.U.A.; Yaqoob, Z.; Nainar, M.A.M.; Razak, S.I.A.; Raza, M.A.; Sajjad, A.; Haider, S.; Busra, F.M. Chitosan/Poly VinylAlcohol/Graphene Oxide BasedpH-Responsive Composite Hydrogel Films: Drug Release, Anti-Microbialand Cell Viability Studies. *Polymers* **2021**, *13*, 3124. [[CrossRef](#)]
38. Han, D.; Yan, L. Supramolecular Hydrogel of Chitosan in the Presence of Graphene Oxide Nanosheets as 2D Cross-Linkers. *ACS Sustain. Chem. Eng.* **2014**, *2*, 296–300. [[CrossRef](#)]
39. Atlan, M.; Neman, J. Targeted Transdermal Delivery of Curcumin for Breast Cancer Prevention. *Int. J. Environ. Res. Public Health* **2019**, *16*, 4949. [[CrossRef](#)]
40. Wong, W.F.; Ang, K.P.; Sethi, G.; Looi, C.Y. Recent Advancement of Medical Patch for Transdermal Drug Delivery. *Medicina* **2023**, *59*, 778. [[CrossRef](#)]
41. Tupal, A.; Sabzichi, M.; Ramezani, F.; Kouhsoltani, M.; Hamishehkar, H. Dermal delivery of doxorubicin-loaded solid lipid nanoparticles for the treatment of skin cancer. *J. Microencapsul.* **2016**, *33*, 372–380. [[CrossRef](#)] [[PubMed](#)]
42. Huwaj, R.A.; Abed, M.; Hamed, R. Innovative transdermal doxorubicin patches prepared using greenly synthesized iron oxide nanoparticles for breast cancer treatment. *Mater. Technol.* **2024**, *39*, 2330278. [[CrossRef](#)]
43. Rajeev, M.R.; Manjusha, V.; Anirudhan, T.S. Transdermal delivery of doxorubicin and methotrexate from polyelectrolyte three-layer nanoparticle of graphene oxide/ polyethyleneimine/ dextran sulphate for chemotherapy: In vitro and in vivo studies. *Chem. Eng. J.* **2023**, *466*, 143244. [[CrossRef](#)]
44. Mohanty, C.; Sahoo, S.K. Curcumin and its topical formulations for wound healing applications. *Drug Discov. Today* **2017**, *22*, 1582. [[CrossRef](#)]
45. Allen, T.M.; Cullis, P.R. Liposomal drug delivery systems: From concept to clinical applications. *Adv. Drug Deliv. Rev.* **2013**, *65*, 36–48. [[CrossRef](#)]
46. Johnsen, K.B.; Gudbergsson, J.M.; Duroux, M.; Moos, T.; Andresen, T.L.; Simonsen, J.B. On the use of liposome controls in studies investigating the clinical potential of extracellular vesicle-based drug delivery systems—A commentary. *J. Control. Release* **2018**, *269*, 10–14. [[CrossRef](#)]
47. Yu, F.; Zhang, Y.; Yang, C.; Li, F.; Qiu, B.; Ding, W. Enhanced transdermal efficiency of curcumin-loaded peptide-modified liposomes for highly effective antipsoriatic therapy. *J. Mater. Chem. B* **2021**, *9*, 4846. [[CrossRef](#)]
48. Zhou, F.; Song, Z.; Wen, Y.; Xu, H.; Zhu, L.; Feng, R. Transdermal delivery of curcumin-loaded supramolecular hydrogels or dermatitis treatment. *J. Mater. Sci. Mater. Med.* **2019**, *30*, 11. [[CrossRef](#)]
49. Suresh, A.B.; Rajeev, M.R.; Anirudhan, T.S. Synthesis of modified tannic acid hydrogel for the transdermal delivery of curcumin. *J. Environ. Chem. Eng.* **2023**, *11*, 109862. [[CrossRef](#)]
50. Mirza, M.A.; Mahmood, S.; Hilles, A.R.; Ali, A.; Khan, M.Z.; Zaidi, S.A.A.; Iqbal, Z.; Ge, Y. Quercetin as a Therapeutic Product: Evaluation of Its Pharmacological Action and Clinical Applications—A Review. *Pharmaceuticals* **2023**, *16*, 1631. [[CrossRef](#)]
51. Ilyich, T.V.; Lapshina, E.A.; Maskevich, A.A.; Veiko, A.G.; Lavysh, A.V.; Palecz, B.; Stepniak, A.; Buko, V.U.; Zavodnik, I.B. Inclusion Complexes of Quercetin with β -Cyclodextrins: Ultraviolet and Infrared Spectroscopy and Quantum Chemical Modeling. *Biophysics* **2020**, *65*, 381. [[CrossRef](#)]

52. Tzankov, B.; Voycheva, C.; Tosheva, A.; Stefanova, D.; Tzankova, V.; Spassova, I.; Kovacheva, D.; Avramova, K.; Tzankova, D.; Yoncheva, K. Novel oleogels for topical delivery of quercetin based on mesoporous silica MCM-41 and HMS particles. *J. Drug Deliv. Sci. Technol.* **2023**, *86*, 104727. [[CrossRef](#)]
53. Vrettos, F.K.; Karouta, N.; Loginos, P.; Donthula, S.; Gournis, D.; Georgakilas, V. The role of diamines in the formation of graphene aerogels. *Front. Mater.* **2018**, *5*, 628–638. [[CrossRef](#)]
54. Liao, Y.; Wang, M.; Chen, D. Preparation of Polydopamine-Modified Graphene Oxide/Chitosan Aerogel for Uranium (VI) Adsorption. *Ind. Eng. Chem. Res.* **2018**, *57*, 8472–8483. [[CrossRef](#)]
55. Taylor, K.; Tabish, T.A.; Narayan, R.J. Drug Release Kinetics of DOX-Loaded Graphene-Based Nanocarriers for Ovarian and Breast Cancer Therapeutics. *Appl. Sci.* **2021**, *11*, 11151. [[CrossRef](#)]
56. Song, J.; Cui, N.; Sun, S.; Lu, X.; Wang, Y.; Shi, H.; Lee, E.S.; Jiang, H.B. Controllability of Graphene Oxide Doxorubicin Loading Capacity Based on Density Functional Theory. *Nanomaterials* **2022**, *12*, 479. [[CrossRef](#)]
57. Some, S.; Gwon, A.-R.; Hwang, E.; Bahn, G.; Yoon, Y.; Kim, Y.; Kim, S.; Bak, S.; Yang, J.; Jo, D.G.; et al. Cancer Therapy Using Ultrahigh Hydrophobic Drug-Loaded Graphene Derivatives. *Sci. Rep.* **2014**, *4*, 6314. [[CrossRef](#)]
58. Cacaci, M.; Squitieri, D.; Palmieri, V.; Torelli, R.; Perini, G.; Campolo, M.; Di Vito, M.; Papi, M.; Posteraro, B.; Sanguinetti, M.; et al. Curcumin-Functionalized Graphene Oxide Strongly Prevents Candida parapsilosis Adhesion and Biofilm Formation. *Pharmaceuticals* **2023**, *16*, 275. [[CrossRef](#)]
59. Madeo, L.F.; Sarogni, P.; Cirillo, G.; Vittorio, O.; Voliani, V.; Curcio, M.; Shai-Hee, T.; Büchner, B.; Mertig, M.; Hampel, S. Curcumin and Graphene Oxide Incorporated into Alginate Hydrogels as Versatile Devices for the Local Treatment of Squamous Cell Carcinoma. *Materials* **2022**, *15*, 1648. [[CrossRef](#)]
60. Croitoru, A.M.; Morosan, A.; Tihauan, B.; Oprea, O.; Motelica, L.; Trusca, R.; Nicoara, A.I.; Popescu, R.C.; Savu, D.; Mihaiescu, D.E.; et al. Novel Graphene Oxide/Quercetin and Graphene Oxide/Juglone Nanostructured Platforms as Effective Drug Delivery Systems with Biomedical Applications. *Nanomaterials* **2022**, *12*, 1943. [[CrossRef](#)] [[PubMed](#)]
61. Brusko, V.; Khannanov, A.; Rakhmatullin, A.; Dimiev, A.M. Unraveling the infrared spectrum of graphene oxide. *Carbon* **2024**, *229*, 119507. [[CrossRef](#)]
62. Khosravi, H.; Naderi, R.; Ramezanzadeh, B. Synthesis and application of molybdate-doped mussel-inspired polydopamine (MI-PDA) biopolymer as an effective sustainable anti-corrosion substance for mild steel in NaCl solution. *Biomass Convers. Biorefinery* **2024**, *14*, 27557–27573. [[CrossRef](#)]
63. Belessi, V.; Petridis, D.; Steriotis, T.; Spyrou, K.; Manolis, G.K.; Psycharis, V.; Georgakilas, V. Simultaneous reduction and surface functionalization of graphene oxide for highly conductive and water dispersible graphene derivatives. *SN Appl. Sci.* **2019**, *1*, 77. [[CrossRef](#)]
64. Li, M.; Miao, Y.; Zhai, X.; Yin, Y.; Zhang, Y.; Jian, Z.; Wang, X.; Sun, L.; Liu, L. Preparation of and research on bioinspired graphene oxide/nanocellulose/polydopamine ternary artificial nacre. *Mater. Des.* **2019**, *181*, 107961. [[CrossRef](#)]
65. Fu, L.; Lai, G.; Jia, B.; Yu, A. Preparation and Electrocatalytic Properties of Polydopamine Functionalized Reduced Graphene Oxide-Silver Nanocomposites. *Electrocatalysis* **2014**, *6*, 1–5. [[CrossRef](#)]
66. Georgitsopoulou, S.; Petrai, O.; Georgakilas, V. Highly conductive functionalized reduced graphene oxide. *Surf. Interfaces* **2019**, *16*, 152–156. [[CrossRef](#)]
67. Georgitsopoulou, S.; Angelopoulou, A.; Papaioannou, L.; Georgakilas, V.; Avgoustakis, K. Self-assembled Janus graphene nanostructures with high camptothecin loading for increased cytotoxicity to cancer cells. *J. Drug Deliv. Sci. Technol.* **2022**, *67*, 102971. [[CrossRef](#)]

Disclaimer/Publisher's Note: The statements, opinions and data contained in all publications are solely those of the individual author(s) and contributor(s) and not of MDPI and/or the editor(s). MDPI and/or the editor(s) disclaim responsibility for any injury to people or property resulting from any ideas, methods, instructions or products referred to in the content.